Phosphorylation-Induced Dimerization of Interferon Regulatory Factor 7 Unmasks DNA Binding and a Bipartite Transactivation Domain

ISABELLE MARIÉ,[1,2] ERIC SMITH,[1] ARUN PRAKASH,[1] AND DAVID E. LEVY[1]*

Department of Pathology and Kaplan Comprehensive Cancer Center, New York University School of Medicine, New York, New York 10016,[1] and Institut Pasteur, 75724 Paris Cedex 15, France[2]

Interferon regulatory factor 7 (IRF7) is an interferon (IFN)-inducible transcription factor required for activation of a subset of IFN-α genes that are expressed with delayed kinetics following viral infection. IRF7 is synthesized as a latent protein and is posttranslationally modified by protein phosphorylation in infected cells. Phosphorylation required a carboxyl-terminal regulatory domain that controlled the retention of the active protein exclusively in the nucleus, as well as its binding to specific DNA target sequences, multimerization, and ability to induce target gene expression. Transcriptional activation by IRF7 mapped to two distinct regions, both of which were required for full activity, while all functions were masked in latent IRF7 by an autoinhibitory domain mapping to an internal region. A conditionally active form of IRF7 was constructed by fusing IRF7 with the ligand-binding and dimerization domain of estrogen receptor (ER). Hormone-dependent dimerization of chimeric IRF7-ER stimulated DNA binding and transcriptional transactivation of endogenous target genes. These studies demonstrate the regulation of IRF7 activity by phosphorylation-dependent allosteric changes that result in dimerization and that facilitate nuclear retention, derepress transactivation, and allow specific DNA binding.

Interferon (IFN) regulatory factors (IRF) are a growing family of transcription factors that have been implicated in antiviral defense, cell growth, and immune regulation (for a review, see reference 30). Nine members of the family have been identified so far: IRF1, IRF2, IRF3, IRF4/Pip/ISCAT, IRF5, IRF6, IRF7, IRF8/ICSBP, and IRF9/ISGF3γ, as well as more distantly related viral IRF homologues encoded by human herpesvirus 8. A hallmark of all of these proteins is a shared sequence homology within the amino-terminal DNA-binding domain (DBD), characterized by a repeat containing five tryptophan residues spaced similarly to the spacing in the DBD of the c-*myb* proto-oncogene (48). This repeat forms a helix-turn-helix motif which determines a characteristic DNA-binding selectivity for GAAA elements (9, 10, 12) found within positive regulatory domain I (PRD I) and PRD III of the IFN-β promoter, the virus-responsive element of the promoters of the IFN-α genes, and the IFN-stimulated response element of IFN-stimulated genes.

In addition to the amino-terminal DBD, IRF proteins contain a carboxyl-terminal effector domain. Sequence conservation within this effector domain allows subclassification of IRF proteins into distinct groups (30). For instance, IRF1 contains a constitutively active transactivation domain within its carboxyl terminus (11) and has been shown to be capable of inducing expression from a variety of target genes containing IRF sites in their promoters (34). IRF2, on the other hand, contains a repression domain and appears to counteract gene expression induced by IRF1 (14), although IRF2 can also activate transcription under certain circumstances (46). The effector domains of all other family members are not intrinsic transactivators but, rather, serve as protein interaction do-

mains to recruit additional transcription factors to promoters containing DNA-bound IRF proteins. For instance, IRF9 (ISGF3γ) recruits tyrosine-phosphorylated STAT1 and/or STAT2 proteins (3, 41, 47) while IRF4 (Pip) and IRF8 (ICSBP) recruit the Ets protein PU.1 (6, 7). This domain, which has been referred to as the IRF association domain (IAD), is capable of mediating dimer formation among IRF partners as well as with heterologous proteins (42), a process that can be influenced by phosphorylation (43). Various IRF family members form homo- or heterodimeric complexes (19, 27, 40), but how this process is regulated and how it influences IRF protein activity has remained unclear.

The involvement of IRF proteins in antiviral responses has prompted interest in how their activity is modulated during viral infection. Inducible phosphorylation of an IRF protein in virus-infected cells was originally suggested for IRF1 (49), and more recently IRF3 and IRF7 have been shown to be phosphorylated specifically after virus infection, leading to induction of IFN-α/β genes or other virus-stimulated genes (1, 15, 22, 23, 25, 29, 31, 37–39, 50, 51, 54). Phosphorylated IRF3 is retained in the nucleus through inactivation of constitutive nuclear export (54), probably due to complex formation with coactivators (20), and becomes bound to DNA as an activator of the immediate-early IFN genes, the IFN-β and IFN-α4 genes, and of additional target genes (22). Similarly, IRF7, which is initially induced in abundance in response to IFN secreted following activation of the immediate-early IFN genes, becomes activated by phosphorylation by a virus-activated protein kinase, leading to a second wave of IFN gene induction from delayed-early genes, such as mouse IFN-α2, IFN-α4, IFN-α6, and IFN-α8 (25, 37) and human IFN-α (52).

In the present study, we have investigated the mechanism of activation of mouse IRF7 during viral infection. Induced phosphorylation of IRF7 led to its homodimerization and to nuclear retention of dimers which were competent to bind DNA and transactivate target genes. Structure-function analysis de-

lineated a strong bipartite transactivation domain which was silenced by an internal autoinhibitory domain that became inactivated following phosphorylation of the carboxyl-terminal regulatory domain. To test the hypothesis that phosphorylation-induced dimerization was the underlying mechanism of IRF7 activation during virus infection, we designed a conditionally dimerized version of IRF7 by fusing it to the ligand-binding domain (LBD) of the estrogen receptor (ER). This domain contains a ligand-dependent dimerization domain (4) that is portable to other proteins (33) and has been used to create conditionally active versions of a variety of proteins, including transcription factors that rely on dimerization for activation (16, 26, 28). IRF7 dimerized through the LBD bound DNA and activated the transcription of endogenous IFN genes in response to hormone treatment in the absence of virus infection, suggesting that the primary function of virus-induced phosphorylation is enhanced dimerization that relieves repression of transactivation imposed by the autoinhibitory domain.

MATERIALS AND METHODS

Cell culture, transfections, and viral infections. Stat1$^{-/-}$ and wild-type immortalized embryo fibroblasts, human embryonic kidney 293T cells, and monkey kidney COS cells were maintained in Dulbecco's modified Eagle's medium supplemented with 10% fetal bovine serum. DNA transfections of 293T, COS, and CV-1 cells and mouse fibroblasts were performed by standard methods using calcium phosphate. All transfection experiments were performed in duplicate, and quantitative data represent the mean normalized for efficiency of transfection and recovery relative to the activity of a cotransfected cytomegalovirus–β-galactosidase construct. Each construct was tested in at least three separate trials, and the trial-to-trial variation was less than 15%. Newcastle disease virus, Manhattan strain (NDV), was grown in 10-day embryonated chicken eggs, and viral infections were performed as previously described (25). Where indicated, cells were treated with IFN-α/β (Lee BioMolecular) at 500 U/ml or with 4-hydroxytamoxifen (4-HT; Sigma) at 1 μM. In the experiments in Fig. 7, the cells were grown in phenol red-free Dulbecco's modified Eagle's medium supplemented with 10% charcoal-stripped, heat-inactivated fetal bovine serum. Polyclonal antisera specific for mouse IRF7 were prepared by immunizing rabbits with glutathione S-transferase fusion protein expressing amino acids 207 to 452 (Zymed). Rabbit and mouse antibodies to Flag were obtained from Zymed and Sigma, respectively, and rat antibodies to HA were obtained from Roche.

Plasmid constructs. The different Gal4-IRF7 chimeras were constructed as follows. The relevant IRF7 segments were generated by PCR and were cloned into the EcoRI and XbaI sites of pSG424 (36) in frame with the Gal4 DBD. The (Gal4)$_5$-luc reporter was kindly provided by T. Hoey (Tularik). Expression and DNA binding of all chimeric constructs were monitored by electrophoretic mobility shift assay (EMSA) using a Gal4-binding-site DNA probe. The deletion mutant Δ238–410 and IRF7-HA were created by recombinant PCR, and the combined fragments were reintroduced into the full-length cDNA cloned in pcDNA3 by using the unique internal restriction site DraIII or BstEII and the XbaI flanking site. Chimeric IRF7-ER was created by replacing the STAT1 coding region in the construct STAT1-ER (28) with the entire coding region of IRF7α or IRF7γ. Details of the reporter construct IFN-α6-luc, the full-length Flag-tagged version of IRF7, and the deletion mutants ΔN^{102} and ΔC^{423} have been reported elsewhere (25). Luciferase activities were measured in cell lysates by using commercial reagents as recommended by the manufacturer (Promega) and were normalized to the β-galactosidase activity of a cotransfected RSV-lacZ plasmid measured on a luminescent substrate (Tropix).

EMSA. Nuclear extracts of transfected 293T cells were prepared as previously described (44). EMSAs were performed by incubating nuclear extracts of each sample (2 μg) with a ^{32}P-labeled double-stranded oligonucleotide containing either three copies of the PRDI-like element from the IFN-α6 promoter (5′-A ATTGAAAGTGAAAAGAAAGTGAAAAGAAAGTGAAAA-3′) or an IFN-stimulated response element sequence derived from the ISG15 gene (21), as previously described (45). 4-HT (1 μM) was added to the DNA-binding reaction mixtures containing IRF7-ER fusion proteins, as previously described (28).

Expression analysis. Quantitative reverse transcription-PCR (RT-PCR) was performed by standard methods using total RNA extracted via the TRIzol method (Life Technologies) and the following primers. To detect the expression of IFN-α genes other than α4, the primers were 5′-ARSYTGTSTGATGCARC AGGT-3′ (sense) and 5′-GGWACACAGTGATCTGTGG-3′ (antisense), and for glyceraldehyde-3-phosphate dehydrogenase the primers were 5′-ACCACA GTCCATGCCATCAC-3′ (sense) and 5′-TCCACCACCCTGTTGCTGTA-3′ (antisense). To estimate relative amounts of specific RNA species, PCRs were performed on serially diluted samples of RT products, as previously described (8).

Isoelectric-focusing analysis. Transfected 293T cells were extracted with RIPA buffer. The samples were immunoprecipitated and analyzed by Western blotting using a precast isoelectric-focusing gel containing a pH gradient from 3 to 10 (Bio-Rad), as recommended by the manufacturer.

Glycerol gradient centrifugation. 293T cells were transfected with expression plasmids encoding IRF7 and were left untreated or infected with NDV 9 h prior to harvest. Nuclear extracts were dialyzed against buffer containing 40 mM KCl, 20 mM HEPES (pH 7.6), 1 mM MgCl$_2$, 0.1 mM EGTA, 0.5 mM dithiothreitol, and 10% glycerol and fractionated on 15 to 30% glycerol gradients by centrifugation, as described previously (18). Fractions were subjected to sodium dodecyl sulfate-polyacrylamide gel electrophoresis (SDS-PAGE) and analyzed by Western blotting using antibodies against IRF7 (Zymed).

RESULTS

Phosphorylated IRF7 accumulates in the nucleus and binds DNA. IRF7 is active only in virus-infected cells (25, 37). To understand how viral infection regulates IRF7 transactivation ability, it was important to ask which characteristics of IRF7 are modified in NDV infected cells. We have previously shown that NDV-induced activation of IRF7 correlated with a shift in its electrophoretic mobility as detected by Western blotting following SDS-PAGE, indicative of protein phosphorylation (25). Analysis of NDV-infected samples by isoelectric focusing confirmed the phosphorylation of IRF7; phosphorylated IRF7 appeared as an extra species that was slightly more acidic than nonphosphorylated IRF7, which displayed a pI of approximately 6.5 (Fig. 1A). Unlike IRF3, which is cytoplasmic until phosphorylation induces nuclear accumulation, latent IRF7 was present in both the cytoplasm and the nucleus (Fig. 1B, lanes 1 and 2). However, the phosphorylated form detected by altered mobility on SDS-PAGE was detected exclusively in the cell nucleus (lane 3). This differential accumulation suggests that NDV-induced phosphorylation of IRF7 results in its retention in the nucleus or that the phosphorylation event itself occurs exclusively in the nucleus. In contrast, bulk IRF7 is not compartmentalized within the cell. However, nuclear localization of phosphorylated IRF7 did not appear to result from inhibited Crm1-dependent nuclear export, as has been suggested for IRF3 nuclear accumulation (54), because leptomycin B treatment of cells did not alter the subcellular distribution of IRF7 (data not shown).

We investigated the aspects of IRF7 function that correlated with its phosphorylation. A dramatically increased ability to bind DNA occurred in response to viral infection (Fig. 1C). Human embryonic kidney 293T cells were transfected with a Flag epitope-tagged version of IRF7, and extracts were prepared before and after infection with NDV. Specific protein-DNA interaction was significantly enhanced in extracts from IRF7-transfected, NDV-infected cells (Fig. 1C, lane 4), and this complex was supershifted by antibody against the epitope tag (lane 5). Consistent with the pattern of nuclear accumulation of phosphorylated protein, DNA-binding-competent IRF7 was selectively detected in nuclear rather than cytoplasmic extracts of infected cells (Fig. 1C, compare lanes 4 and 7). These data demonstrated that the phosphorylated form of IRF7 is competent to bind DNA and accumulates selectively in the nucleus.

IRF7 contains a bipartite transactivation domain whose activity is controlled by an autoinhibitory domain. During the initial characterization of IRF7 cDNA clones, we isolated several isoforms derived by alternative splicing (unpublished data). Major forms expressed in mouse fibroblasts included IRF7α, an apparently full-length transcript, along with two smaller species, IRF7β and IRF7γ, lacking internal portions of the protein encoded by exons 4 and 5 (Fig. 2A). We tested the ability of these different IRF7 isoforms to activate an IFN-α6
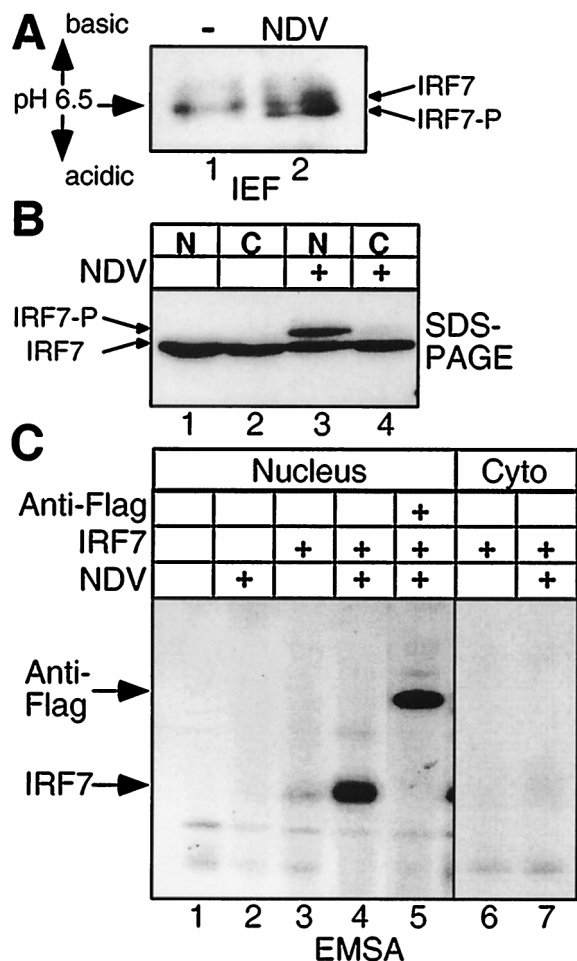
FIG. 1. Phosphorylated IRF7 accumulates in the nucleus and binds DNA. (A) Isoelectric-focusing analysis of NDV-activated IRF7. 293T cells were transfected with an IRF7-HA expression plasmid. At 16 h post-transfection, cells were mock infected (lane 1) or NDV infected (lane 2) for 7 h and cell extracts were immunoprecipitated and analyzed by native isoelectric focusing and Western blotting using anti-HA antibodies. The mobilities of IRF7 and phosphorylated IRF7 (IRF7-P) are indicated. (B) Phosphorylated IRF7 is exclusively nuclear. 293T cells were transfected with an IRF7 expression plasmid, and nuclear (N) and cytoplasmic (C) extracts prepared from mock- or NDV-infected cells 9 h postinfection were analyzed by Western blotting using anti-IRF7 antibodies raised against the carboxyl terminus. The mobilities of IRF7 and phosphorylated IRF7 (IRF7-P) are indicated. (C) IRF7 binds DNA in response to viral infection. EMSA was performed on nuclear (lanes 1 to 5) and cytoplasmic (lanes 6 and 7) extracts derived from vector-transfected 293T cells (lanes 1 and 2) or cells expressing IRF7-Flag (lanes 3 to 7) that had been mock or NDV infected for 9 h, as indicated. Extracts were incubated with an ISRE probe from the ISG15 gene. Anti-Flag M2 antibodies were added to the reaction mixture (lane 5) to confirm the identity of the complex.

luciferase reporter. As described previously (25), full-length IRF7α potently transactivated the IFN-α6 promoter in response to viral infection (Fig. 2A). IRF7β was also capable of activating the IFN-α6 promoter in response to NDV, but to levels approximately twofold lower than those for IRF7α. In contrast, IRF7γ, which has sustained a larger deletion than IRF7α and IRF7β, was incapable of inducing NDV-responsive transcription (Fig. 2A), although it still underwent a size shift following virus infection, indicative of phosphorylation (data not shown). These results suggest that amino acids 132 to 205, which are differentially contained within the distinct IRF7 isoforms, are essential for transactivation and may comprise a

transactivation domain. Similarly, deletion of the carboxyl-terminal region necessary for virus-induced phosphorylation (ΔC^{423}) severely impaired IRF7 transcriptional potency (Fig. 2A), suggesting that this region also contains an essential transactivation function. To test the importance of the remaining portion of the IRF7 carboxyl terminus, we constructed an artificial deletion mutant missing amino acids 238 to 410 (Fig. 2A, Δ$^{238-410}$). Surprisingly, the protein encoded by this construct constitutively activated the IFN-α6 promoter to high levels and failed to respond further to virus infection. These data delineate two regions necessary for full transcriptional activity (amino acids 132 to 205 and 423 to 457) and an additional autoinhibitory region that silences transcriptional activity in the absence of viral infection (amino acids 238 to 410).

The transactivation potential of IRF7Δ$^{238-410}$ was tested at various expression levels to determine if its high activity indicated saturation of the expression assay. Titration of the amount of IRF7 DNA cotransfected with IFN-α6-luc resulted in a proportional decrease of the transcriptional response (Fig. 2B). For instance, transfection of fivefold-lower amounts of IRF7Δ$^{238-410}$ relative to IRF7α constitutively induced reporter gene expression approximately equal to virus-induced wild-type levels. However, virus infection did not significantly alter reporter gene activity at any level of IRF7Δ$^{238-410}$ expression (Fig. 2B and data not shown), demonstrating that its enhanced activity was not responsive to regulation. We considered the possibility that the high activity resulting from absence of the autoinhibitory region might reflect constitutive phosphorylation of the regulatory region (e.g., due to increased access to a regulatory kinase or lack of a potentially inactivating dephosphorylation event). This notion was tested by expressing IRF7Δ$^{238-410}$(AA), in which two serine residues required for virus-induced phosphorylation were altered to alanines (25). This altered protein retained the potent transactivating ability and lack of significant viral responsiveness of the nonmutated version (Fig. 2C). These data argue that the sole effect of virus infection-induced regulation is derepression of transactivation by inactivation of the autoinhibitory region, a requirement that is lost when autoinhibition is eliminated by deletion of the relevant domain.

Domain organization of IRF7. The data reported above suggested that IRF7 contains two regions necessary for transcriptional activity flanking an autoinhibitory segment that silences transcription in the absence of viral infection. This notion was further investigated by using a fusion protein approach. For this purpose, we subcloned different segments of IRF7 in frame with the yeast Gal4 DBD in the pSG424 vector (36). The transactivation ability of these chimeric Gal4-IRF7 proteins was tested by cotransfection into COS cells using a reporter gene containing five Gal4-binding sites upstream of the luciferase coding region.

A chimeric protein containing full-length IRF7 (amino acids 1 to 457) fused to the Gal4 DBD stimulated transcription approximately 100-fold relative to the Gal4 DBD alone (Fig. 3A), demonstrating that IRF7 is a functional transcriptional activator. Similarly, expression of a fusion protein containing amino acids 132 to 457 but lacking the putative IRF7 DBD also activated the Gal4-responsive promoter greater than 300-fold. These results confirm that the carboxyl terminus of IRF7 contains all the elements necessary for transactivation, similar to other IRF family members (30). To dissect the transactivation domain, amino acids 424 to 457 were deleted from the carboxyl terminus, similar to the ΔC423 mutant, which showed impaired virus response. This deletion also showed reduced transcription as a Gal4 fusion. This impaired transcription was not affected by loss of elements within the amino-terminal DBD,
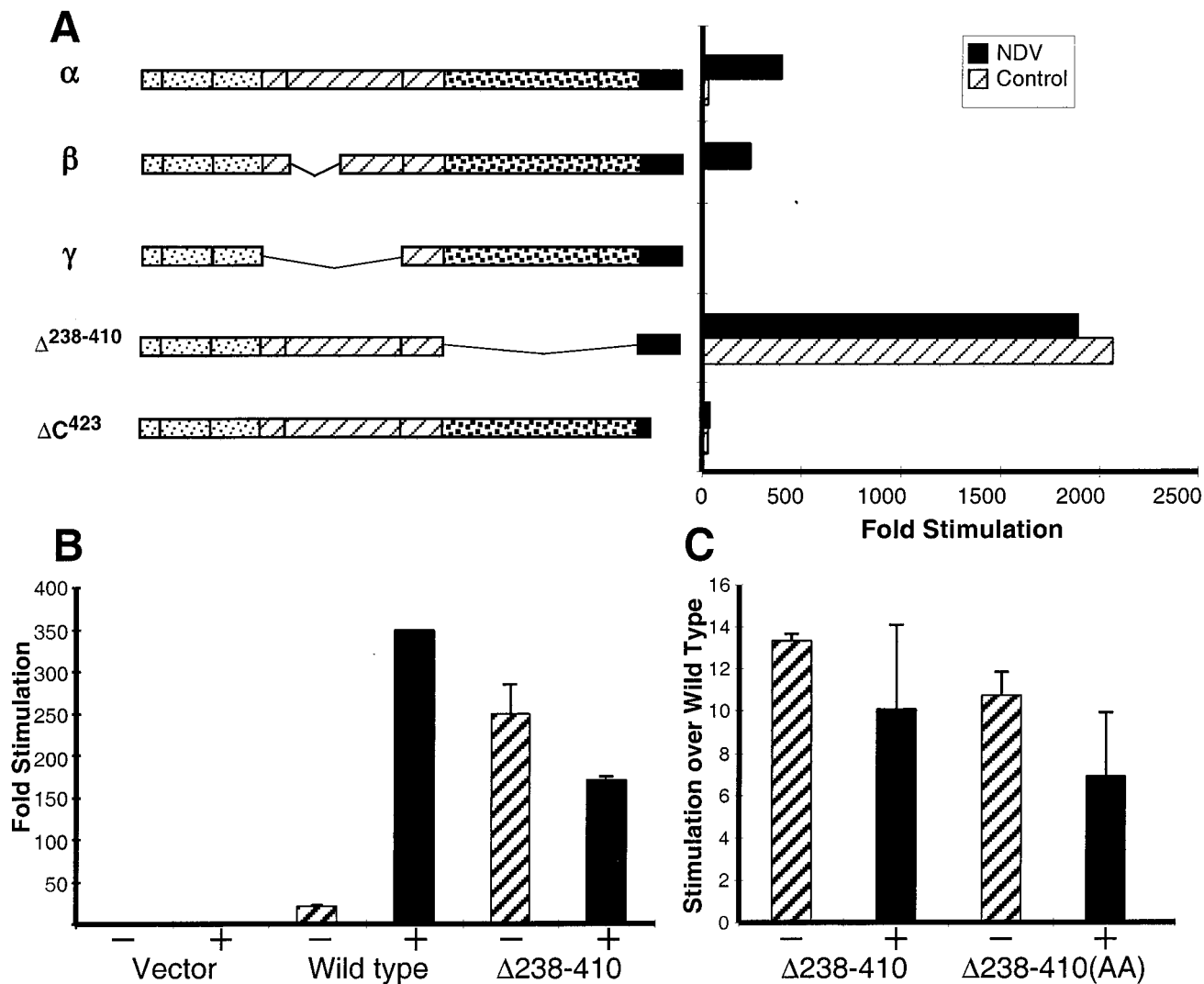
FIG. 2. Transactivation of the IFN-α6 promoter by IRF7. (A) COS cells were transfected with the diagrammed IRF7 splice variant and truncation mutant expression constructs along with a luciferase reporter driven by the IFN-α6 promoter. At 24 h after transfection, cells were mock infected (hatched bars) or infected with NDV for 12 h (solid bars) before being assayed for luciferase activity. The values are expressed as fold induction relative to cells transfected with empty vector after normalization to cotransfected β-galactosidase. Mean values from a single representative experiment performed in duplicate are shown. Each construct was tested in at least three separate experiments, and variation between experiments was less than 10%. (B) IRF7$\Delta^{238-410}$ lacking the autoinhibitory domain does not respond to viral infection. COS cells were transfected and treated as in panel A, except that fivefold less IRF7$\Delta^{238-410}$ DNA was transfected relative to wild-type IRF7. (C) IRF7$\Delta^{238-410}$ does not require phosphorylation regulatory sequences for constitutive transcriptional activity. Cells were transfected with IRF7$\Delta^{238-410}$ or with IRF7$\Delta^{238-410}$ in which the two serine residues required for phosphorylation of the regulatory domain were converted to alanines (AA). Data are expressed as fold activation of the IFN-α6-luc reporter relative to its activation by virus-activated wild-type IRF7.

because a similar chimeric molecule containing amino acids 132 to 424 but missing the carboxyl-terminal 34 amino acids also failed to activate transcription to wild-type levels. Further carboxyl-terminal truncation to amino acid 367 produced a protein completely lacking the ability to activate transcription, confirming that a necessary transactivation domain exists at the extreme carboxyl terminus of IRF7. Indeed, the carboxyl-terminal transactivation region alone (amino acids 411 to 457) was also capable of stimulating high levels of transcription when expressed as a Gal4 fusion (Fig. 3A, construct 11), demonstrating that this segment contained a bona fide transactivation function.

Further truncations to produce chimeric proteins expressing amino acids 132 to 237 or 132 to 205 resulted in proteins capable of strongly stimulating transcription by more than 200-

and 100-fold, respectively, identifying the second region capable of activating transcription. To map this second region, constructs expressing amino acids 153 to 457 or 207 to 457 were tested and found not to be capable of activating transcription. These results localized the second transactivation domain between amino acids 132 and 237 and confirmed that its activity in the intact protein is inhibited by the presence of amino acids 238 to 410. Removal of the internal transactivation region in the context of the rest of the carboxyl-terminus of IRF7 (e.g., amino acids 153 to 457 or 207 to 457) significantly impaired transcription, showing that both the internal and the distal transactivation regions were essential for full activity. Interestingly, combining the internal transactivation domain with the carboxyl-terminal region in the absence of the autoinhibitory segment ($\Delta^{238-410}$) produced an extremely active
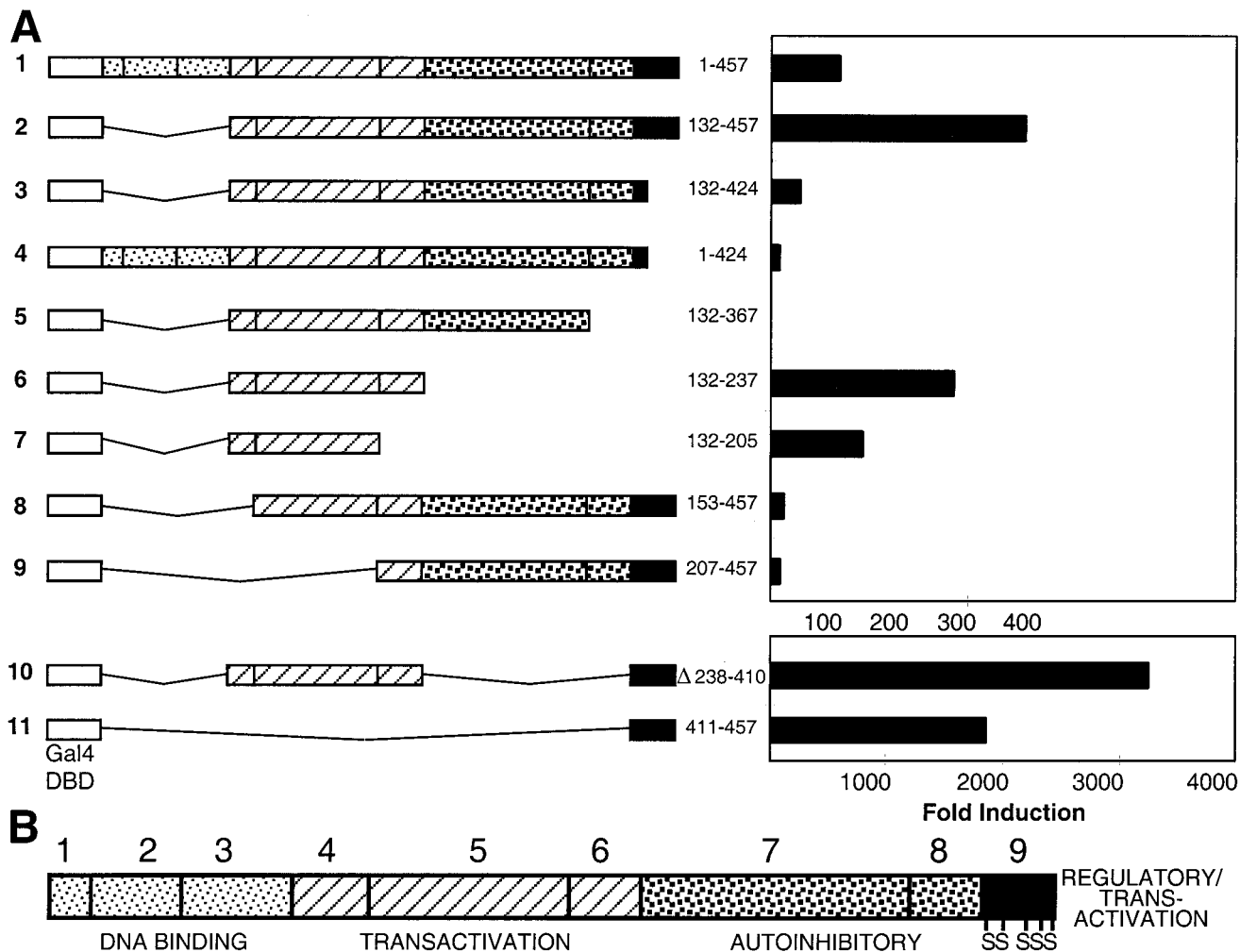
FIG. 3. Structure-function mapping of IRF7 transactivation and autoinhibitory domains using Gal4 chimeras. Gal4-IRF7 fusion protein constructs are diagrammed on the left, indicating the Gal4 DBD and the exon structure of IRF7. Distinct functional regions of IRF7 are shaded. Fold activation of a Gal4 upstream activation site luciferase reporter cotransfected in COS cells with the indicated Gal4-IRF7 chimeric expression plasmids is shown on the right. The values are expressed as fold induction relative to basal activation by Gal4-DBD alone after normalization to cotransfected β-galactosidase activity. The graph represents the mean value from a single experiment performed in duplicate and is representative of at least three trials for each construct. Overall experimental variation was consistently less than 15%. Note that the results for constructs 1 to 9 and 10 to 11 are plotted on different scales. (B) Diagram of IRF7 functional domains, indicated by different shading patterns and labeled underneath, summarizing the data derived from transfection experiments. Exons are numbered for identification.

protein that stimulated transcription to levels approximately 10-fold higher than those for full-length IRF7. Taken together with the studies of the activation of the IFN-α6 reporter (Fig. 2), these results demonstrate that amino acids 238 to 410 function in an autoinhibitory manner to silence the two separate parts of the transactivation domain. Deletion of either region (internal or distal) of the transactivation domain in the context of at least part of the autoinhibitory segment resulted in a very poor transactivation ability (e.g., Fig. 3, constructs 5 and 9), while removal of the inhibitory region in the context of either transactivation domain resulted in high levels of transcription (constructs 6, 7, 10, and 11).

It is important to note that the carboxyl-terminal region containing an independent transactivation function and necessary for full transcriptional activity of intact IRF7 also contains serine residues required for phosphorylation in response to NDV infection and necessary for regulated induction of endogenous IFN-α genes (25). Constructs that retained this region (e.g., Fig. 3, constructs 1 and 2) consistently showed a two-

to threefold increase in transactivation following viral infection (data not shown), indicating that the chimeric Gal4 proteins retained at least partial responsiveness to virus infection-dependent regulation.

Taken together, the above results map the distinct functional domains of IRF7 as diagrammed in Fig. 3B. The DBD is at the amino terminus (A. Prakash, unpublished data), probably encoded by the first 3 exons. A region necessary for transactivation lies between amino acids 132 and 237, and this region is differentially spliced in IRF7α, IRF7β, and IRF7γ isoforms. A similar region of human IRF7 has also been implicated in transactivation (1). An autoinhibitory domain capable of silencing the activity of both of the otherwise constitutively active transactivation domains mapped between amino acids 238 and 410, and the extreme carboxyl terminus of IRF7 is required for full transactivation and in addition serves as a virus-activated regulatory domain. Phosphorylation of the regulatory domain derepresses transactivation by inactivating the inhibition imposed by the autoinhibitory domain, and the require-
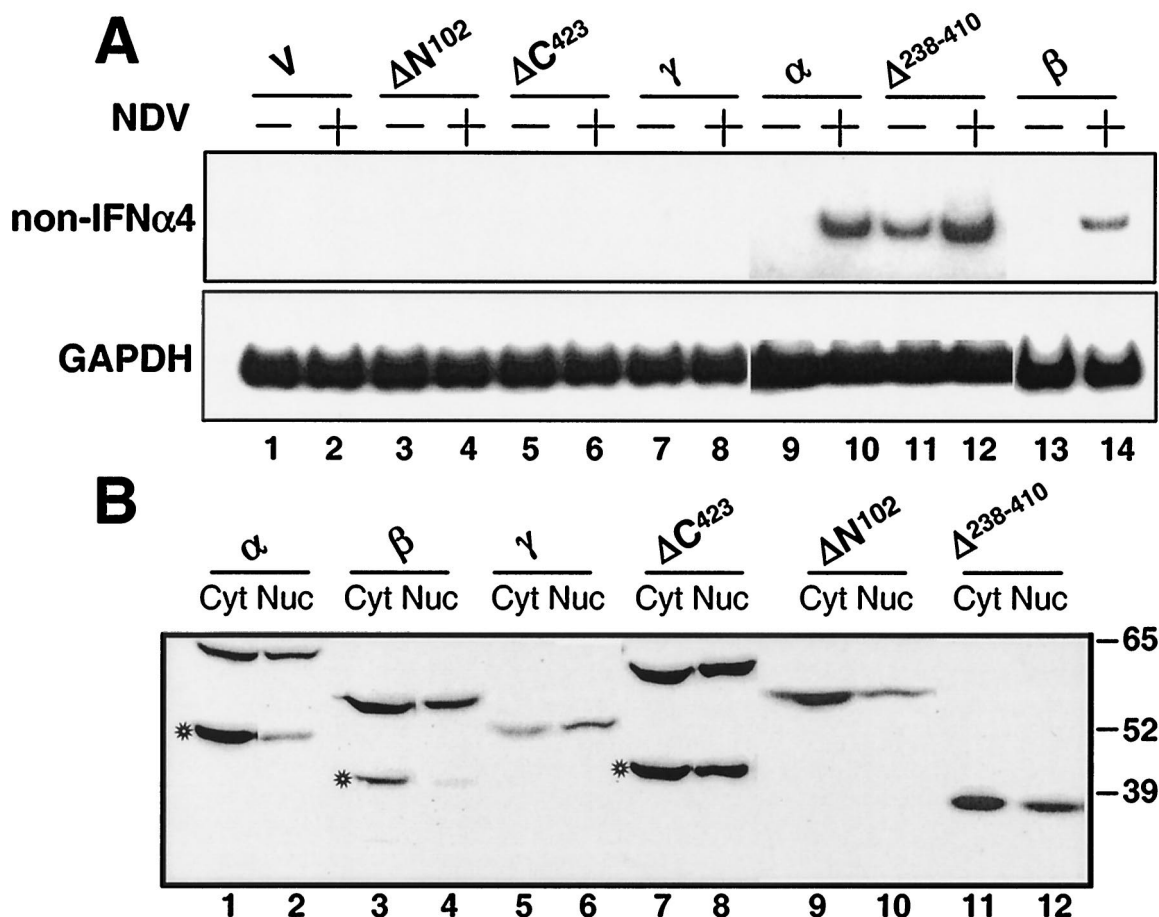
FIG. 4. Induction of endogenous IFN-α gene expression by IRF7 isoforms. (A) Stat1$^{-/-}$ fibroblasts were transiently transfected with expression plasmids encoding IRF7 splice variants and truncation mutants, as indicated. After 36 h, cells were mock or NDV infected for 9 h and levels of non-IFN-α4 and GAPDH mRNA were monitored by RT-PCR, as indicated. (B) IRF7 accumulates in both the cytoplasm and nucleus. Expression levels of each IRF7 splice variant or truncation mutant in extracts from transiently transfected cells were monitored by Western blotting. The faster-migrating forms observed in lanes 1, 3, 7, and 8 (indicated by ∗) are most probably proteolytic breakdown products. The mobilities of molecular mass markers are indicated on the right in kilodaltons.

ment for this regulatory function is lost following removal of the autoinhibitory region.

Induction of endogenous IFN gene expression by relief of IRF7 autoinhibition. The subset of IFN-α genes not including IFN-α4 is induced in a delayed manner following virus infection and requires IRF7 for expression, as previously described (1, 25, 52). Because IRF7 must be induced in response to IFN, IRF7-dependent targets such as the non-IFN-α4 subset fail to be induced in virus-infected IFN-resistant cells, such as Stat1$^{-/-}$ cells (25). This property afforded the unique opportunity to confirm the domain mapping of IRF7 originally carried out using transfected reporters on endogenous IFN-α genes. To this end, we examined the expression of non-IFN-α4 genes in virus-infected Stat1$^{-/-}$ fibroblasts transfected with different versions of recombinant IRF7 (Fig. 4A). Vector-transfected cells or cells ectopically expressing IRF7 versions lacking either the DBD (ΔN^{102}) or the carboxyl-terminal transactivation/regulatory domain (ΔC^{423}) were incapable of activating endogenous IFN-α gene expression in response to virus infection (Fig. 4A, lanes 1 to 6). Similarly, IRF7γ, which lacks most of the internal transactivation domain, failed to complement Stat1$^{-/-}$ cells (lanes 7 and 8). However, consistent with reporter assay results, both IRF7α and the IRF7β splice variant missing a small segment of the internal transactivation

domain were functional, although IRF7β was less active than IRF7α (compare lanes 10 and 14), resulting in approximately 5- to 10-fold less gene expression as quantified by titration RT-PCR (data not shown). All forms of IRF7 were expressed at comparable levels and, like full-length IRF7, accumulated in both the cytoplasm and nucleus (Fig. 4B). While IRF7γ expression levels were lower than others, this reduced accumulation did not account for the observed complete absence of IFN gene induction.

In contrast to the deficiencies in endogenous IFN gene induction observed following transfection of impaired versions of IRF7, the Δ$^{238-410}$ construct, which lacked the autoinhibitory domain, induced IFN-α gene expression even in the absence of NDV infection (Fig. 4A, lanes 11 and 12). Similar to its increased activity as a Gal4 fusion and its constitutive induction of IFN-α6-luc, IRF7Δ$^{238-410}$ induced constitutive endogenous IFN-α gene expression. Interestingly, although IRF7Δ$^{238-410}$ displayed enhanced basal activity consistent with results obtained using artificial promoters, NDV infection of IRF7Δ$^{238-410}$ transfected cells further enhanced the levels of target gene expression (Fig. 4A, compare lanes 11 and 12). This result is in contrast to IRF7Δ$^{238-410}$ activity in transient-luciferase assays (Fig. 2). It is likely that this virus-induced activation reflects the increased complexity of endogenous gene regulation relative to

reporter assays. For instance, induction of IFN-α/β mRNA levels reflects both transcriptional activation of gene expression and posttranscriptional events, including a significant contribution of enhanced IFN mRNA stability following virus infection (Y. L. Yang and C. Weissmann, personal communication). In addition, virus infection may produce changes in chromatin structure that affect the expression of endogenous genes that are not required in simpler reporter assays. In this regard, it is noted that the non-IFN-α4 genes are located within the same chromosomal cluster as the immediate-early IFN-α4 and IFN-β genes (17) and therefore may be affected by their actively transcribed neighbors, a regulatory event that would not be reflected by reporter constructs.

IRF7γ represses NDV-induced IFN-α expression. The fact that IRF7γ was devoid of transactivation ability prompted us to ask whether this splice variant could have a repressive effect on IRF7 transactivation. Cotransfection experiments were performed using increasing amounts of IRF7γ and a reporter construct encoding the luciferase gene driven by the IFN-α6 promoter activated by either IRF7α or IRF7β in response to viral infection (Fig. 5, upper panels). Expression of IRF7γ repressed IRF7α- or IRF7β-driven transactivation by more than 90% at high molar ratios. Even at low ratios, expression of IRF7γ negatively affected IRF7α- or IRF7β-mediated target gene activation. IRF7γ-mediated repression was more effective against IRF7β, probably due to the weaker transcriptional potential of the β isoform. These results indicated that the naturally occurring IRF7γ splice variant could function as an antagonist of IRF7α or IRF7β to modulate the transcription of IRF7-dependent genes.

Several possible mechanisms for this dominant negative action of IRF7γ are imaginable. First, because it contains a DBD, IRF7γ could compete with active forms of IRF7 for promoter-binding sites. Second, heterodimerization between active and inactive forms of IRF7 might prevent the formation of functional homodimers possibly required for gene induction. Third, IRF7γ might interact with other necessary components of the transcriptional machinery and sequester a protein essential for IRF7 activity. To distinguish among these different possibilities, we tested another IRF7 mutant for possible dominant negative properties. Similar cotransfection experiments were performed using IRF7ΔN^{102}, which lacks the amino-terminal DBD, rendering it unable to bind DNA (data not shown). As shown in Fig. 5 (lower panels), this mutant also functioned in a dominant negative manner, inhibiting IRF7α- and IRF7β-mediated transactivation of the IFN-α6 promoter by up to 80%. Since this mutant cannot bind DNA, its inhibitory action strongly suggests a repression mechanism that is independent of competition for DNA binding. Alternatively, it is possible that IRF7γ and IRF7ΔN^{102} inhibit IRF7 action through distinct mechanisms. However, deletion of amino acids 58 to 73 within the DBD of IRF7γ, rendering it incapable of binding DNA, did not prevent its dominant negative effect in cotransfection assays (data not shown).

Enhanced IRF7 dimerization following viral infection. A likely mechanism for the dominant negative action of IRF7γ would be the formation of nonfunctional dimers with IRF7α, suggesting that active IRF7α exists as a dimer. To address the possibility of IRF7 dimerization, the native sizes of nonphosphorylated and phosphorylated IRF7 were determined by glycerol gradient centrifugation. Nuclear extracts from uninfected or NDV-infected cells were fractionated by sedimentation, and the relative mass of IRF7 was estimated following Western blotting. As shown in Fig. 6 (upper panel), nonphosphorylated IRF7 derived from uninfected cells cofractionated with the 44-kDa marker, approximating its predicted size. Similarly, the

bulk of nonphosphorylated IRF7 derived from infected cells (lower panel) cosedimented with IRF7 derived from uninfected cells, accumulating in fractions 7 and 8. A similar pattern of sedimentation was observed for cytoplasmic IRF7, whether derived from uninfected or virus-infected cells (data not shown). In contrast, phosphorylated IRF7, which migrated more slowly on SDS-PAGE and was detected exclusively in nuclear extracts from infected cells, sedimented with a significantly larger apparent size, with peak accumulation detected in fraction 10 (Fig. 6, lower panel). This faster sedimentation of phosphorylated IRF7 was consistent with a size of 80 to 90 kDa. It is unlikely that a conformational change in phosphorylated IRF7 monomers could account for this significantly faster sedimentation, suggesting instead that phosphorylated IRF7 is not a monomer.

Dimerization is sufficient to activate IRF7. The significantly larger native size of phosphorylated IRF7 suggested that dimerization might be key to its infection-dependent activation. To test the notion that homodimerization per se would suffice to activate IRF7, we designed conditionally dimerizable forms by fusing IRF7 to the LBD of ER (IRF7-ER), as diagrammed in Fig. 7A. The effectiveness of hormone in stably dimerizing and activating the chimeric IRF7α-ER protein was tested by induction of gene expression. Activation of target gene expression by the chimeric IRF7α-ER protein was tested on the IFN-α6 promoter by cotransfection of COS cells with IRF7α-ER and IFN-α6-luc, followed by hormone stimulation (Fig. 7B). The ER LBD carries one of the two transactivation functions of the wild-type receptor, namely, AF-2 (13). While estradiol is a full agonist for ER and can activate the function of AF-2, giving some degree of transactivation even in the absence of the major transactivation domain of the receptor, tamoxifen is an antagonist which fails to activate AF-2 function although it retains the ability to induce ER dimerization (2). To test exclusively the transactivation function of IRF7 rather than AF-2 from ER, transfected cells were stimulated with 4-HT. IRF7α-ER stimulated with 4-HT resulted in greater than 25-fold activation of the reporter, showing that ligand-induced dimerization was sufficient for transcriptional activation. As expected, 4-HT had no effect on reporter expression in the absence of IRF7α-ER. To prove definitively that the AF-2 domain from ER was not responsible for the induction of transcription observed in response to 4-HT, a second IRF7-ER fusion construct was prepared using IRF7γ that lacks the internal transactivation domain. IRF7γ-ER-transfected cells treated with 4-HT resulted in only minimal induction of the IFN-α6-luc reporter (Fig. 7B), even though both IRF7α-ER and IRF7γ-ER chimeric proteins were expressed at comparable levels and bound DNA (Fig. 7D and E). Therefore, the AF-2 domain of ER was insufficient to contribute to reporter gene expression following 4-HT treatment.

The ER LBD not only functions as a dimerization domain but also can inactivate heterologous fusion proteins through interaction with HSP90 (33), leading to the possibility that hormone activation of IRF7α-ER resulted from release from HSP90 rather than from true activation. To test this possibility, we compared gene activation by wild-type (unactivated) IRF7 with that of IRF7-ER activated by 4-HT. If the action of hormone were merely to release basal IRF7 from HSP90-mediated inhibition rather than to activate it, one would expect 4-HT-activated transcription to equal that from unphosphorylated, wild-type IRF7. Transient transfection of cells with IRF7 produced a small increase in IFN-α6-luc expression relative to NDV-induced levels (Fig. 7C). However, 4-HT-activated IRF7α-ER produced significantly higher target gene expression than did wild-type IRF7α alone, resulting in transcrip-
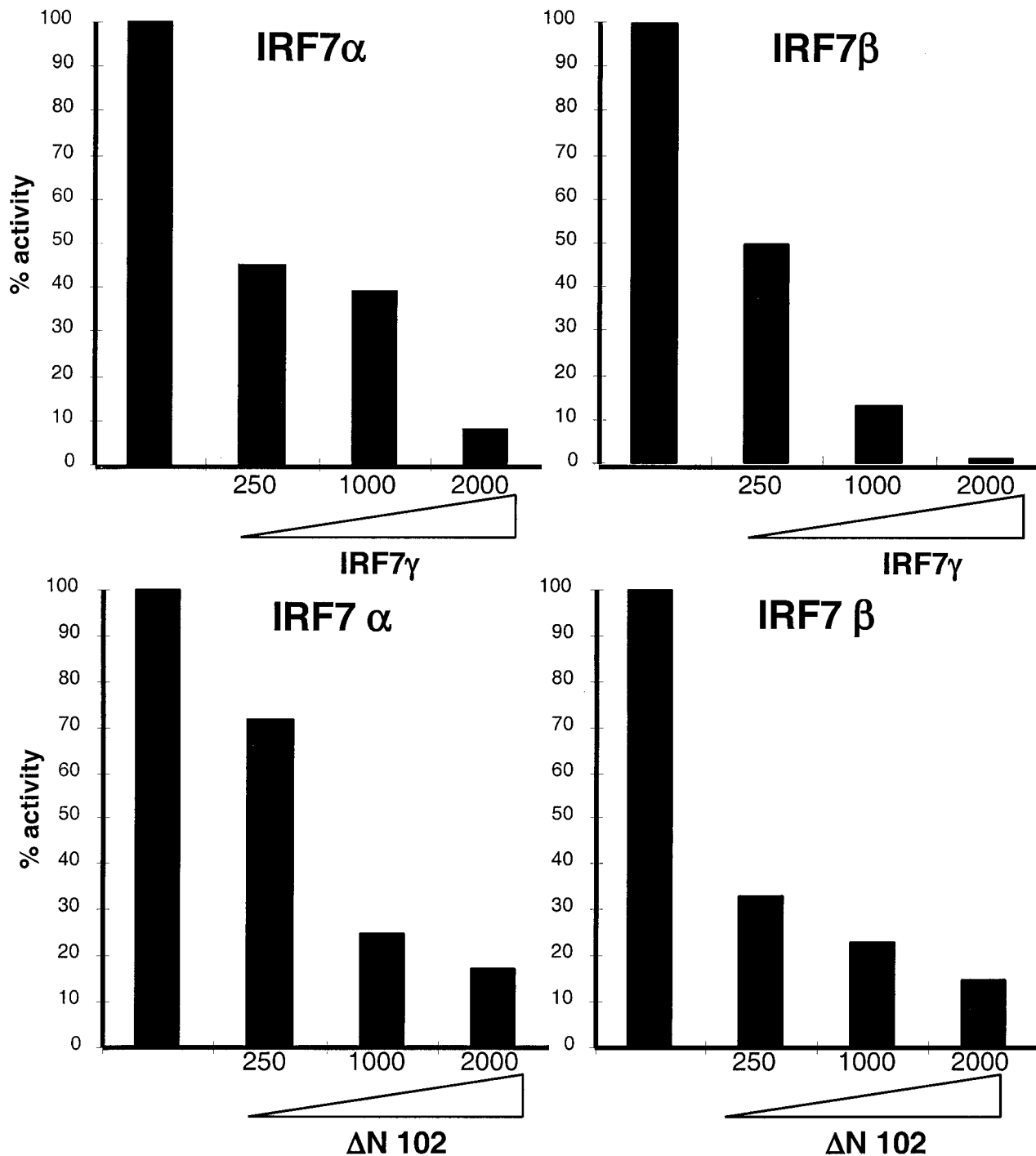
FIG. 5. IRF7γ and IRF7ΔN^{102} competitively repress IRF7-mediated IFN-α6 induction. COS cells were cotransfected with expression constructs encoding IRF7α or IRF7β (50 ng), as indicated, and increasing amounts (0, 250, 1,000, and 2,000 ng) of either IRF7γ (upper panels) or IRF7ΔN^{102} (lower panels), along with a luciferase reporter construct driven by the IFN-α6 promoter. At 24 h after transfection, cells were infected with NDV for 12 h and extracts were assayed for luciferase activity. The values are expressed as a percentage of the activity without competitor after normalization to cotransfected β-galactosidase activity and represent the average of duplicate measurements.

tional activation equal to approximately half that of NDV-induced wild-type protein. Therefore, the action of hormone cannot be ascribed to release from HSP90 alone. Another potential confounding variable could be that 4-HT treatment resulted in phosphorylation and thereby activation of IRF7-

ER, analogous to NDV-induced phosphorylation. To test this possibility, a third ER fusion protein was constructed in which serine residues 425 and 426, required for virus-induced activation of IRF7, were converted to alanines (25). Cells transfected with this mutated construct (AA-ER) showed increased re-
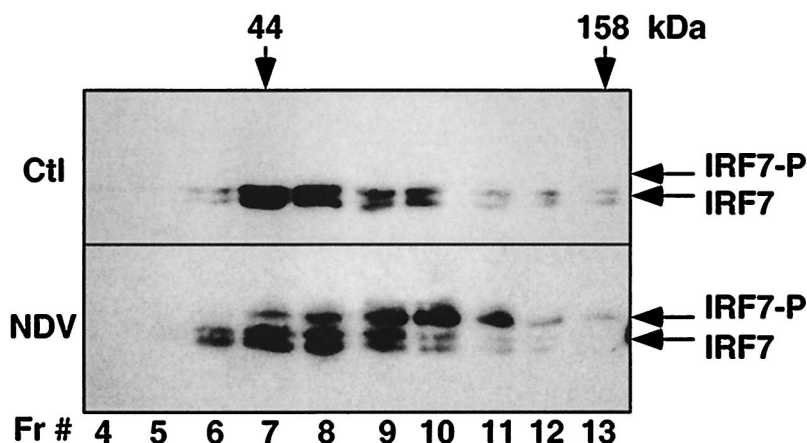
FIG. 6. Phosphorylated IRF7 displays an increased native molecular size. Nuclear extracts harvested from uninfected control (Ctl) (upper panel) or NDV-infected (lower panel) 293T cells that had been transfected with IRF7 were fractionated by glycerol gradient sedimentation. Individual fractions, as indicated, were assayed for IRF7 by immunoblotting following SDS-PAGE. The fractionation of molecular mass standards in a parallel gradient is indicated at the top, and the electrophoretic mobilities of phosphorylated and unphosphorylated IRF7 are indicated at the right.

porter gene expression following treatment with 4-HT (Fig. 7C). Although gene induction by the AA-ER protein was somewhat lower than that by unmutated IRF7α-ER, it was nonetheless greater than gene induction in response to unphosphorylated, wild-type IRF7. Moreover, treatment of cells with 4-HT after transfection with wild-type IRF7 showed no increase in gene expression, and no evidence of phosphorylation of either wild-type IRF7 or IRF7-ER was detected (data not shown).

Ligand-activated IRF7 was also tested for induction of specific DNA binding. Cells transfected with IRF7α-ER were treated with 4-HT and cell extracts were examined for binding to an IRF7-binding site DNA probe (Fig. 7E). As expected, no specific DNA-binding activities were detected from extracts of cells transfected with vector alone or with wild-type IRF7, either with or without hormone treatment (data not shown). However, cells expressing IRF7α-ER and treated with 4-HT displayed a characteristic DNA-protein complex (lane 2). IRF7α-ER retained the binding specificity of wild-type IRF7 and could be recovered from nuclear extracts of hormone-treated cells (results not shown). Similarly, 4-HT induced the DNA-binding ability of IRF7γ-ER (lane 4). Thus, dimerization through the ER moiety mimicked both of the major regulated events normally dependent on viral infection-induced phosphorylation, namely, DNA binding and gene activation.

The ability of hormone-dimerized IRF7 to regulate target gene transcription was confirmed by evaluation of endogenous IFN gene expression. Stat1$^{-/-}$ fibroblasts were transfected with IRF7-ER and left untreated or stimulated with 4-HT, and induced mRNA levels of type I IFN genes were measured. As shown in Fig. 7F, 4-HT treatment was capable of inducing expression of the non-IFN-α4 subset in IRF7α-ER-transfected cells (lane 2). In contrast, hormone did not induce IFN-α in cells transfected with the transcriptionally impaired IRF7γ-ER construct (lane 4) or with wild-type IRF7 (not shown). Therefore, dimerization of IRF7 through the ER domain was sufficient to induce the expression of the IRF7-dependent subset of endogenous IFN-α/β genes in the absence of phosphorylation but dependent on the IRF7 TAD, consistent with dimerization playing a key role in derepressing the DNA-binding and transcriptional activation functions of this transcription factor.

DISCUSSION

Our experiments have focused on understanding the structural determinants underlying the transcriptional activity of IRF7 and the mechanism of its regulation during viral infection. We showed that murine IRF7 contains a transactivation function composed of two distinct stretches of amino acids, separated by an autoinhibitory segment capable of silencing its activity. The same autoinhibitory segment appears capable of preventing DNA binding by latent IRF7. Upon viral infection, IRF7 phosphorylated within the carboxyl-terminal regulatory domain forms stable multimers, most probably composed of homodimers, and this form accumulates preferentially in the nucleus, where it binds specific DNA motifs and enhances the transcription of target genes. All of the features of IRF7 associated with virus-induced activity, namely, nuclear accumulation of the active form, ability to bind DNA, and ability to induce gene expression of specific endogenous target genes, could be mimicked by forced dimerization through the ER LBD. These results show that phosphorylation-dependent dimerization of IRF7 in virus infected cells is the likely mechanism regulating its function.

Our data support the hypothesis that dimerization alone, in the absence of phosphorylation or other viral infection-induced events, is sufficient to confer all the features of IRF7 activation: nuclear retention, specific DNA binding, and transcriptional competence, including induction of endogenous target genes. It is important to note that the ER LBD used in these experiments provides a hormone-regulated dimerization function but lacks the key nuclear localization signals present in wild-type ER (32, 53). Therefore, ligand-dependent nuclear migration of IRF7-ER demonstrates that IRF7-encoded signals are sufficient for nuclear localization, although the precise mechanism driving nuclear retention of dimeric IRF7 remains to be determined. Furthermore, the hormone-binding domain of ER contains only one of the two independent transcriptional activation functions present in intact ER, namely, AF-2 (13). While estradiol is a full agonist for ER and can activate AF-2 function, tamoxifen has no ability to activate AF-2 function, although it retains the ability to induce ER dimerization (2). Importantly, tamoxifen activated IRF7 target gene expression in cells transfected with IRF7α-ER (Fig. 7) but not in cells
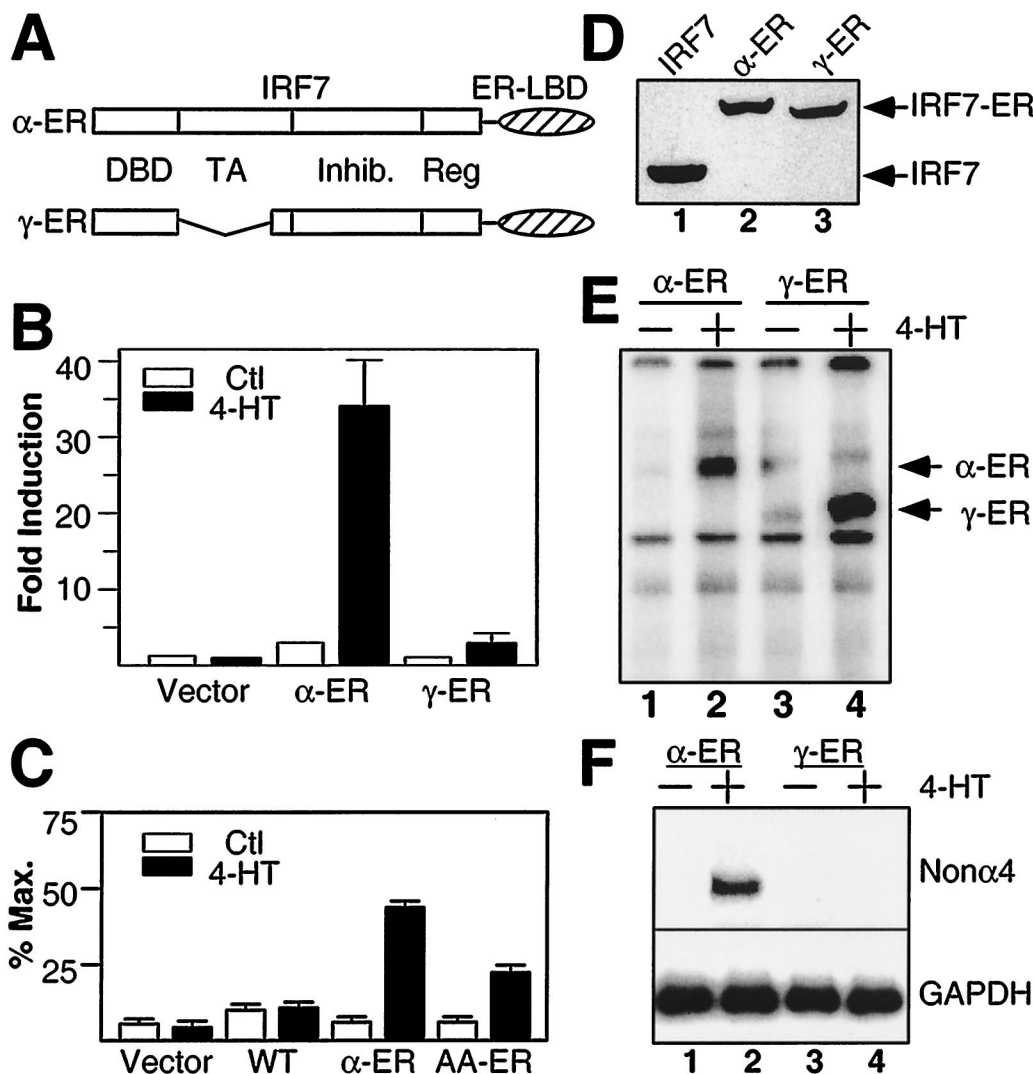
FIG. 7. Hormone-dependent dimerization of IRF7-ER induces specific DNA binding and IFN-α gene expression. (A) Diagram of the IRF7-ER chimeric proteins. The DBD, transactivation domain (TA), autoinhibitory domain (Inhib.), regulatory domain (Reg), and estrogen LBD are indicated for IRF7α (upper) and the IRF7γ splice variant (lower). (B) 293T cells were cotransfected with IFN-α6-luc plus vector, IRF7α-ER, or IRF7γ-ER, as indicated, and then treated for 16 h with 4-HT or left untreated (Ctl) before being assayed for luciferase activity. Data are shown as fold induction over untreated, vector-transfected cells and represent the mean and standard error of duplicate measurements. (C) Cells cotransfected with IFN-α6-luc plus vector, wild-type IRF7α, IRF7α-ER, or IRF7α(AA)-ER were left untreated or treated for 16 h with 4-HT before being assayed for luciferase activity. Data are shown as percent maximal activity obtained in NDV-infected cells transfected with wild-type IRF7 (results not shown) and represent the mean and standard error of triplicate determinations. (D) IRF7α (lane 1), IRF7α-ER (lane 2), and IRF7γ-ER (lane 3) protein levels were measured in extracts from transfected 293T cells by immunoblotting. (E) Extracts of cells transfected with IRF7α-ER (α-ER) or IRF7γ-ER (γ-ER), as indicated, that had been left untreated (lanes 1 and 3) or treated for 4 h with 4-HT (lanes 2 and 4) were analyzed by EMSA. The positions of the IRF7-ER protein-DNA complexes are indicated. (F) Stat1$^{-/-}$ fibroblasts were transfected with IRF7α-ER (lanes 1 and 2) or IRF7γ-ER (lanes 3 and 4) before being treated with 4-HT for 6 h (even-numbered lanes). RNA was analyzed for expression of the non-IFN-α4 subset or for GAPDH, as indicated.

expressing the transcriptionally impaired IRF7γ-ER protein. Therefore, the IRF7-encoded transactivation function was both necessary and sufficient to induce gene expression once activated through dimerization.

The multiple regulated activities of IRF7 dependent on phosphorylation of the carboxyl-terminal regulatory domain suggest that this modification is accompanied by major structural reorganization of the protein following dimerization. It is possible that internal interactions of the nonphosphorylated protein keep it in a "closed" conformation that prevents DNA binding and blocks the formation and/or the function of the transactivation domain. One possibility is that the inhibited state is a consequence of an intramolecular interaction, as

postulated for IRF4 and IRF3 (5, 24). Our results suggest that such an interaction probably involves amino acids 131 to 205, the region absent in IRF7γ, since this splice variant displayed constitutive DNA binding (unpublished data). Unlike IRF3, however, acquisition of DNA binding was not sufficient to activate transcription, even though the carboxyl-terminal transactivation domain was still present in IRF7γ, because the presence of the autoinhibitory domain prevented activity from both portions of the transactivation domain. We speculate that dimerization relieves a negative interaction between the internal transactivation region and the DBD, perhaps as a concerted effect of creating a functional transactivation domain by uniting the internal and distal portions.

Many of these features are similar to the regulation of the related protein IRF3, which is also activated during viral infection by phosphorylation (15, 23, 24, 29, 35, 38, 39, 50, 51, 54). Our data show that, at least for IRF7, the mechanism underlying the regulation of its activity is induced dimerization that derepresses its ability to bind DNA and transactivate gene expression, actions that are silenced in the latent protein. It is tempting to speculate that other family members, in particular IRF3, are regulated through a similar dimerization-dependent mechanism. Both IRF3 and IRF7 are transcriptional activators, containing transactivation domains masked in the absence of phosphorylation by autoinhibitory domains. Moreover, regulatory phosphorylation requires an analogous and partially homologous region at the carboxyl termini of the two proteins. However, IRF3 contains a single region (amino acids 134 to 394) required for transactivation, flanked by two autoinhibitory domains (24). In contrast, IRF7 contains two regions necessary for full transactivation (one from amino acids 132 to 238 and a segment distal to amino acid 423), separated by a single autoinhibitory region. It is interesting that two related proteins that exhibit structural divergence in the sequence and placement of functional domains nevertheless retain a similar overall regulatory mechanism.

Another major difference between IRF3 and IRF7 is the inducibility of IRF7 protein abundance in response to IFN, in contrast to the constitutive expression of IRF3, providing a unique aspect of cellular regulation. Moreover, while both proteins are regulated by subcellular distribution, IRF3 is excluded from the nucleus in the absence of viral infection due to active nuclear export (54). In contrast, the distribution of bulk IRF7 was similar in both cytoplasmic and nuclear compartments, with only the phosphorylated form specifically accumulating in the nucleus. This regulation does not appear to be dependent on active nuclear export since the inhibition of Crm1-dependent export by leptomycin B did not lead to accumulation of IRF7 in the nucleus (data not shown). Au et al. (1) reported that a transiently transfected human IRF7-green fluorescent protein fusion accumulated over time in the nucleus, even in the absence of viral infection. In contrast, Sato et al. (37) found that epitope-tagged IRF7 protein expressed from a retrovirus accumulated in the nucleus only in response to virus. Importantly, however, we examined the distribution of endogenous IRF7 in several cell lines and found that endogenous IRF7 protein was present in both cytoplasmic and nuclear compartments while endogenous IRF3 was predominantly or exclusively cytoplasmic (data not shown), indicating that the detected pattern of subcellular compartmentalization is not an artifact of transfected cells. Therefore, while phosphorylation of IRF3 appears to mask its nuclear export signal, leading to its accumulation in the nucleus, phosphorylation of IRF7 either occurs only in the nucleus or modulates subcellular localization by a distinct mechanism. In either case, functional dimerization appears to be the fundamental consequence of phosphorylation that alters IRF7 subcellular localization since hormone-activated IRF7-ER also accumulated in the nucleus.

Another distinction between the two proteins is the presence of alternatively spliced versions of IRF7 that specifically remove different segments of the internal transactivation domain. Interestingly, IRF7β, which is a weaker transactivator than IRF7α and is more easily inhibited by IRF7γ, appears to be the predominant form expressed in many cells, including leukocytes (data not shown), raising the possibility that negative regulation by IRF7γ inhibition could be a significant mechanism in vivo. While we have not detected conditions in vivo in which IRF7γ is the predominant species, it is possible that the relative abundance of IRF7β and IRF7γ may affect the magnitude of target gene induction and that modulation of these levels could provide an additional level of gene regulation. Perhaps more importantly, however, the ability of IRF7γ to inhibit transcriptional activity provided strong evidence that dimerization is key to IRF7 function.

All IRF family proteins appear to be organized in the same general manner, containing an amino-terminal DBD specific for a conserved ISRE/PRDI-like DNA sequence and a carboxyl-terminal effector domain that includes the IAD and that functions by protein-protein interaction (43). For instance, IRF9 (ISGF3γ p48) uses this domain to interact with STAT1 and STAT2 in response to IFN stimulation (47), while IRF4 (Pip) and IRF8 (ICSBP) interact with phosphorylated PU.1 (5) or with IRF1 and IRF2 (40, 43) through the IAD. IRF3, IRF4, and IRF7 appear to use the IAD both for intramolecular autoinhibitory interactions and to form an intermolecular, activated conformation. Most IRF proteins have been suggested to dimerize and/or multimerize (19). The identification regulated dimerization as underlying mechanism of functional activation, as demonstrated here for IRF7, may be generally applicable for other members of the family.

REFERENCES

1. **Au, W. C., P. A. Moore, D. W. LaFleur, B. Tombal, and P. M. Pitha.** 1998. Characterization of the interferon regulatory factor-7 and its potential role in the transcription activation of interferon A genes. J. Biol. Chem. **273:** 29210–29217.
2. **Berry, M., D. Metzger, and P. Chambon.** 1990. Role of the two activating domains of the oestrogen receptor in the cell-type and promoter-context dependent agonistic activity of the anti-oestrogen 4-hydroxytamoxifen. EMBO J. **9:**2811–2818.
3. **Bluyssen, H. A. R., R. Muzaffar, R. J. Vliestra, A. C. J. van der Made, S. Leung, G. R. Stark, I. M. Kerr, J. Trapman, and D. E. Levy.** 1995. Combinatorial association and abundance of interferon-stimulated gene factor 3 components dictate the selectivity of interferon responses. Proc. Natl. Acad. Sci. USA **92:**5645–5649.
4. **Brandt, M. E., and L. E. Vickery.** 1997. Cooperativity and dimerization of recombinant human estrogen receptor hormone-binding domain. J. Biol. Chem. **272:**4843–4849.
5. **Brass, A. L., E. Kehrli, C. F. Eisenbeis, U. Storb, and H. Singh.** 1996. Pip, a lymphoid-restricted IRF, contains a regulatory domain that is important for autoinhibition and ternary complex formation with the Ets factor PU.1. Genes Dev. **10:**2335–2347.
6. **Brass, A. L., A. Q. Zhu, and H. Singh.** 1999. Assembly requirements of PU.1-Pip (IRF-4) activator complexes: inhibiting function in vivo using fused dimers. EMBO J. **18:**977–991.
7. **Eisenbeis, C. F., H. Singh, and U. Storb.** 1995. Pip, a novel IRF family member, is a lymphoid-specific, Pu.1-dependent transcriptional activator. Genes Dev. **9:**1377–1387.
8. **Erlandsson, L., R. Blumenthal, M. L. Eloranta, H. Engel, G. Alm, S. Weiss, and T. Leanderson.** 1998. Interferon-beta is required for interferon-alpha production in mouse fibroblasts. Curr. Biol. **8:**223–226.
9. **Escalante, C. R., J. Yie, D. Thanos, and A. K. Aggarwal.** 1998. Structure of IRF-1 with bound DNA reveals determinants of interferon regulation. Nature **391:**103–106.
10. **Fujii, Y., T. Shimizu, M. Kusumoto, Y. Kyogoku, T. Taniguchi, and T.**

Hakoshima. 1999. Crystal structure of an IRF-DNA complex reveals novel DNA recognition and cooperative binding to a tandem repeat of core sequences. EMBO J. **18:**5028–5041.

11. **Fujita, T., Y. Kimura, M. Miyamoto, E. L. Barsoumian, and T. Taniguchi.** 1989. Induction of endogenous IFN-alpha and IFN-beta genes by a regulatory transcription factor, IRF-1. Nature **337:**270–272.

12. **Furui, J., K. Uegaki, T. Yamazaki, M. Shirakawa, M. B. Swindells, H. Harada, T. Taniguchi, and Y. Kyogoku.** 1998. Solution structure of the IRF-2 DNA-binding domain: a novel subgroup of the winged helix-turn-helix family. Structure **6:**491–500.

13. **Gronemeyer, H.** 1991. Transcription activation by estrogen and progesterone receptors. Annu. Rev. Genet. **25:**89–123.

14. **Harada, H., T. Fujita, M. Miyamoto, Y. Kimura, M. Maruyama, A. Furia, T. Miyata, and T. Taniguchi.** 1989. Structurally similar but functionally distinct factors, IRF-1 and IRF-2, bind to the same regulatory elements of IFN and IFN-inducible genes. Cell **58:**729–739.

15. **Juang, Y., W. Lowther, M. Kellum, W. C. Au, R. Lin, J. Hiscott, and P. M. Pitha.** 1998. Primary activation of interferon A and interferon B gene transcription by interferon regulatory factor 3. Proc. Natl. Acad. Sci. USA **95:**9837–9842.

16. **Kamogawa, Y., H. J. Lee, J. A. Johnston, M. McMahon, A. O'Garra, and N. Arai.** 1998. A conditionally active form of STAT6 can mimic certain effects of IL-4. J. Immunol. **161:**1074–1077.

17. **Kelley, K. A., and P. M. Pitha.** 1985. Characterization of a mouse interferon gene locus I. Isolation of a cluster of four alpha interferon genes. Nucleic Acids Res. **13:**805–823.

18. **Kessler, D. S., S. A. Veals, X. Y. Fu, and D. E. Levy.** 1990. IFN-alpha regulates nuclear translocation and DNA-binding affinity of ISGF3, a multimeric transcriptional activator. Genes Dev. **4:**1753–1765.

19. **Kirchhoff, S., F. Schaper, A. Oumard, and H. Hauser.** 1998. In vivo formation of IRF-1 homodimers. Biochimie **80:**659–664.

20. **Kumar, K. P., K. M. McBride, B. K. Weaver, C. Dingwall, and N. C. Reich.** 2000. Regulated nuclear-cytoplasmic localization of interferon regulatory factor 3, a subunit of double-stranded RNA-activated factor 1. Mol. Cell. Biol. **20:**4159–4168.

21. **Levy, D. E.** 1998. Analysis of interferon-regulated proteins binding the interferon-alpha-stimulated response element. Methods **15:**167–174.

22. **Lin, R., C. Heylbroeck, P. Genin, P. M. Pitha, and J. Hiscott.** 1999. Essential role of interferon regulatory factor 3 in direct activation of RANTES chemokine transcription. Mol. Cell. Biol. **19:**959–966.

23. **Lin, R., C. Heylbroeck, P. M. Pitha, and J. Hiscott.** 1998. Virus-dependent phosphorylation of the IRF-3 transcription factor regulates nuclear translocation, transactivation potential, and proteasome-mediated degradation. Mol. Cell. Biol. **18:**2986–2996.

24. **Lin, R., Y. Mamane, and J. Hiscott.** 1999. Structural and functional analysis of interferon regulatory factor 3: localization of the transactivation and autoinhibitory domains. Mol. Cell. Biol. **19:**2465–2474.

25. **Marié, I., J. E. Durbin, and D. E. Levy.** 1998. Differential viral induction of distinct interferon-alpha genes by positive feedback through interferon regulatory factor-7. EMBO J. **17:**6660–6669.

26. **Matsuda, T., T. Nakamura, K. Nakao, T. Arai, M. Katsuki, T. Heike, and T. Yokota.** 1999. STAT3 activation is sufficient to maintain an undifferentiated state of mouse embryonic stem cells. EMBO J. **80:**4261–4269.

27. **Meraro, D., S. Hashmueli, B. Koren, A. Azriel, A. Oumard, S. Kirchhoff, H. Hauser, S. Nagulapalli, M. L. Atchison, and B. Z. Levi.** 1999. Protein-protein and DNA-protein interactions affect the activity of lymphoid-specific IFN regulatory factors. J. Immunol. **163:**6468–6478.

28. **Milocco, L. H., J. A. Haslam, J. Rosen, and H. M. Seidel.** 1999. Design of conditionally active STATs: insights into STAT activation and gene regulatory function. Mol. Cell. Biol. **19:**2913–2920.

29. **Navarro, L., K. Mowen, S. Rodems, B. Weaver, N. Reich, D. Spector, and M. David.** 1998. Cytomegalovirus activates interferon immediate-early response gene expression and an interferon regulatory factor 3-containing interferon-stimulated response element-binding complex. Mol. Cell. Biol. **18:**3796–3802.

30. **Nguyen, H., J. Hiscott, and P. M. Pitha.** 1997. The growing family of interferon regulatory factors. Cytokine Growth Factor Rev. **8:**293–312.

31. **Parekh, B. S., and T. Maniatis.** 1999. Virus infection leads to localized hyperacetylation of histones H3 and H4 at the IFN-beta promoter. Mol. Cell **3:**125–129.

32. **Picard, D., V. Kumar, P. Chambon, and K. R. Yamamoto.** 1990. Signal transduction by steroid hormones: nuclear localization is differentially regulated in estrogen and glucocorticoid receptors. Cell Regul. **1:**291–299.

33. **Picard, D., S. J. Salser, and K. R. Yamamoto.** 1988. A movable and regulable

34. **Pine, R.** 1992. Constitutive expression of an ISGF2/IRF1 transgene leads to interferon-independent activation of interferon-inducible genes and resistance to virus infection. J. Virol. **66:**4470–4478.

35. **Ronco, L. V., A. Y. Karpova, M. Vidal, and P. M. Howley.** 1998. Human papillomavirus 16 E6 oncoprotein binds to interferon regulatory factor-3 and inhibits its transcriptional activity. Genes Dev. **12:**2061–2072.

36. **Sadowski, I., and M. Ptashne.** 1989. A vector for expressing GAL4(1-147) fusions in mammalian cells. Nucleic Acids Res. **17:**7539.

37. **Sato, M., N. Hata, M. Asagiri, T. Nakaya, T. Taniguchi, and N. Tanaka.** 1998. Positive feedback regulation of type I IFN genes by the IFN-inducible transcription factor IRF-7. FEBS Lett. **441:**106–110.

38. **Sato, M., N. Tanaka, N. Hata, E. Oda, and T. Taniguchi.** 1998. Involvement of the IRF family transcription factor IRF-3 in virus-induced activation of the IFN-beta gene. FEBS Lett. **425:**112–116.

39. **Schafer, S. L., R. Lin, P. A. Moore, J. Hiscott, and P. M. Pitha.** 1998. Regulation of type I interferon gene expression by interferon regulatory factor-3. J. Biol. Chem. **273:**2714–2720.

40. **Schaper, F., S. Kirchhoff, G. Posern, M. Koster, A. Oumard, R. Sharf, B. Z. Levi, and H. Hauser.** 1998. Functional domains of interferon regulatory factor I (IRF-1). Biochem. J. **335:**147–157.

41. **Seegert, D., I. Strehlow, B. Klose, D. E. Levy, C. Schindler, and T. Decker.** 1994. A novel IFN-α-regulated DNA-binding protein participates in the regulation of the IFP53/tryptophanyl-tRNA synthetase gene. J. Biol. Chem. **269:**8590–8595.

42. **Sharf, R., A. Azriel, F. Lejbkowicz, S. S. Winograd, R. Ehrlich, and B. Z. Levi.** 1995. Functional domain analysis of interferon consensus sequence binding protein (ICSBP) and its association with interferon regulatory factors. J. Biol. Chem. **270:**13063–13069.

43. **Sharf, R., D. Meraro, A. Azriel, A. M. Thornton, K. Ozato, E. F. Petricoin, A. C. Larner, F. Schaper, H. Hauser, and B. Z. Levi.** 1997. Phosphorylation events modulate the ability of interferon consensus sequence binding protein to interact with interferon regulatory factors and to bind DNA. J. Biol. Chem. **272:**9785–9792.

44. **Silvennoinen, O., J. N. Ihle, J. Schlessinger, and D. E. Levy.** 1993. Interferon-induced nuclear signaling by Jak protein tyrosine kinases. Nature **366:**583–585.

45. **Silvennoinen, O., C. Schindler, J. Schlessinger, and D. E. Levy.** 1993. Ras-independent signal transduction in response to growth factors and cytokines by tyrosine phosphorylation of a common transcription factor. Science **261:**1736–1739.

46. **Vaughan, P. S., A. J. van Wijnen, J. L. Stein, and G. S. Stein.** 1997. Interferon regulatory factors: growth control and histone gene regulation—it's not just interferon anymore. J. Mol. Med. **75:**348–359.

47. **Veals, S. A., T. Santa Maria, and D. E. Levy.** 1993. Two domains of ISGF3gamma that mediate protein-DNA and protein-protein interaction during transcription factor assembly contribute to DNA-binding specificity. Mol. Cell. Biol. **13:**196–206.

48. **Veals, S. A., C. Schindler, D. Leonard, X. Y. Fu, R. Aebersold, J. E. Darnell, and D. E. Levy.** 1992. Subunit of an alpha-interferon-responsive transcription factor is related to interferon regulatory factor and myb families of DNA-binding proteins. Mol. Cell. Biol. **12:**3315–3324.

49. **Watanabe, N., J. Sakakibara, A. G. Hovanessian, T. Taniguchi, and T. Fujita.** 1991. Activation of IFN-beta element by IRF-1 requires a posttranslational event in addition to IRF-1 synthesis. Nucleic Acids Res. **19:**4421–4428.

50. **Wathelet, M. G., C. H. Lin, B. S. Parekh, L. V. Ronco, P. M. Howley, and T. Maniatis.** 1998. Virus infection induces the assembly of coordinately activated transcription factors on the IFN-β enhancer in vivo. Mol. Cell **1:**507–518.

51. **Weaver, B. K., K. P. Kumar, and N. C. Reich.** 1998. Interferon regulatory factor 3 and CREB-binding protein/p300 are subunits of double-stranded RNA-activated transcription factor DRAF1. Mol. Cell. Biol. **18:**1359–1368.

52. **Yeow, W. S., W. C. Au, Y. T. Juang, C. D. Fields, C. L. Dent, D. R. Gewert, and P. M. Pitha.** 2000. Reconstitution of virus-mediated expression of interferon alpha genes in human fibroblast cells by ectopic interferon regulatory factor-7. J. Biol. Chem. **275:**6313–6320.

53. **Ylikomi, T., M. T. Bocquel, M. Berry, H. Gronemeyer, and P. Chambon.** 1992. Cooperation of proto-signals for nuclear accumulation of estrogen and progesterone receptors. EMBO J. **11:**3681–3694.

54. **Yoneyama, M., W. Suhara, Y. Fukuhara, M. Fukuda, E. Nishida, and T. Fujita.** 1998. Direct triggering of the type I interferon system by virus infection: activation of a transcription factor complex containing IRF-3 and CBP/p300. EMBO J. **17:**1087–1095.

inactivation function within the steroid binding domain of the glucocorticoid receptor. Cell **54:**1073–1080.